

Fundamental limits on the rate of bacterial cell division

Nathan M. Belliveau^{1, *}, Griffin Chure^{2, 3, *}, Christina L. Hueschen⁴, Hernan G. Garcia⁵, Jané Kondev⁶, Julie Theriot^{1, 7}, Rob Phillips^{1, 8, †}

*For correspondence:

[†]These authors contributed equally to this work

¹Department of Biology, University of Washington, Seattle, WA, USA; ²Division of Biology and Biological Engineering, California Institute of Technology, Pasadena, CA, USA; ³Department of Applied Physics, California Institute of Technology, Pasadena, CA, USA; ⁴Department of Chemical Engineering, Stanford University, Stanford, CA, USA; ⁵Department of Molecular Cell Biology and Department of Physics, University of California Berkeley, Berkeley, CA, USA; ⁶Department of Physics, Brandeis University, Waltham, MA, USA; ⁷Allen Institute for Cell Science, Seattle, WA, USA; ⁸Department of Physics, California Institute of Technology, Pasadena, CA, USA; [†]Address correspondence to phillips@pboc.caltech.edu; *Contributed equally

Abstract

Introduction

The range of bacterial growth rates can be enormous. In natural environments, doublings occur approximately once per year whereas in comfortable laboratory conditions, growth can be rapid with several divisions per hour. This remarkable diversity illustrates the intimate relationship between environmental conditions and the rates at which cells convert nutrients into new cellular material. This relationship between the environment and cellular growth rate has remained a major topic of inquiry in bacterial physiology for over a century (*Jun et al., 2018*). In 1958, Schaecter, Malløe, and Kjeldgaard reported the discovery of a strong, linear dependence of the total cellular protein content on the growth rate, revealing a fundamental relationship between the environment and the composition of the intracellular milieu (*Schaechter et al., 1958*). Over the past decade, a remarkable body of work has examined this relationship with single-protein resolution using modern methods of mass spectrometry (*Valgepea et al., 2013; Peebo et al., 2015; Schmidt et al., 2016*) and ribosomal profiling (*Li et al., 2014*) which permit a quantitative investigation of the relationship between gene expression and growth rate. This body of experimental data places us in the auspicious position to explore how the abundance of fundamental protein complexes are related to the growth rate of the population and interrogate what biological processes may set the speed limit of bacterial growth.

In this work, we seek to leverage a collection of proteomic data sets of *Escherichia coli* across 31 growth conditions to quantitatively explore what biological processes may set the speed limit of bacterial growth. Broadly speaking, we entertain several classes of hypotheses as are illustrated in *Figure 1*. First, we consider potential limits on the transport of nutrients into the cell. We address this hypothesis by performing an order-of-magnitude estimate for how many carbon atoms needed to facilitate this requirement given a 6000 second division time. As a second hypothesis, we consider there exists a fundamental limit on how quickly the cell can generate ATP. We approach this hypothesis from two angles, considering how many ATP synthase complexes must be needed

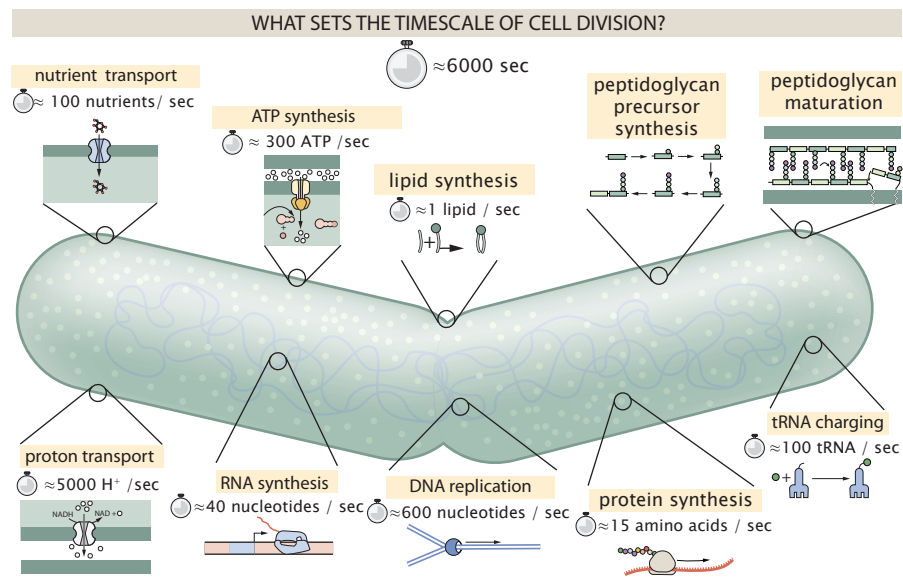


Figure 1. Transport and synthesis processes necessary for cell division. We consider an array of processes necessary for a cell to double its molecular components. Such processes include the transport of carbon across the cell membrane, the production of ATP, and fundamental processes of the central dogma namely RNA, DNA, and protein synthesis. A schematic of each synthetic or transport category is shown with an estimate of the rate per macromolecular complex. In this work, we consider a standard bacterial division time of ≈ 6000 sec.

to churn out enough ATP to power protein translation followed by an estimation of how many electron transport complexes must be present to maintain the proton motive force. Our third and final class of hypotheses centers on the synthesis of a variety of biomolecules. Our focus is primarily on the stages of the central dogma as we estimate the number of protein complexes needed for DNA replication, transcription, and protein translation.

With estimates in hand for each of these processes, we turn to our collection of data sets to assess the accuracy of our estimates. In broad terms, we find that the majority of our estimates are exceeded by the experimental observations, allowing us to systematically scratch off the hypotheses diagrammed in **Figure 1** as setting the speed limit. Ultimately, we find that protein translation (particularly the generation of new ribosomes) acts as the rate limiting step of bacterial division. We again leverage the quantitative nature of this data set and present a quantitative model of the relationship between the fraction of the proteome devoted to ribosomes and the speed limit of translation, revealing a fundamental tradeoff between the translation capacity of the ribosome pool and the maximal cellular growth rate.

Nutrient Transport

In order to build new cellular mass, the molecular and elemental building blocks must be scavenged from the environment in different forms. Carbon, for example, is acquired via the transport of carbohydrates and sugar alcohols with some carbon sources receiving preferential treatment in their consumption (*Monod, 1947*). Phosphorus, sulfur, and nitrogen, on the other hand, are harvested primarily in the forms of inorganic salts, namely phosphate, sulfate, and ammonia (*Jun et al., 2018; Assentoft et al., 2016; Stasi et al., 2019; Antonenko et al., 1997; Rosenberg et al., 1977; Willsky et al., 1973*). All of these compounds have different permeabilities across the cell membrane and most require some energetic investment either via ATP hydrolysis or through the proton electrochemical gradient to bring the material across the hydrophobic cell membrane. Given the diversity of biological transport mechanisms and the vast number of inputs needed to build a cell, we begin by considering transport of elemental requirements as a possible rate-limiting step

of bacterial cell division.

The elemental composition of *E. coli* has received much quantitative attention over the past half century (Neidhardt *et al.*, 1991; Taymaz-Nikerel *et al.*, 2010; Heldal *et al.*, 1985; Bauer and Ziv, 1976), providing us a starting point for estimating the copy numbers of various transporters. While there is some variability in the exact elemental percentages (with different uncertainties), we can estimate that the dry mass of a typical *E. coli* cell is $\approx 45\%$ carbon (BNID: 100649, Milo *et al.* (2010)), $\approx 15\%$ nitrogen (BNID: 106666, Milo *et al.* (2010)), $\approx 3\%$ phosphorus (BNID: 100653, Milo *et al.* (2010)), and 1% sulfur (BNID: 100655, Milo *et al.* (2010)). In the coming paragraphs, we will examine how many transporters and/or channels must be present to maintain these elemental compositions with a moderate doubling time of 6000 s.

Carbon Transport

We begin with the most abundant element by mass, carbon. Using ≈ 0.3 pg as the typical *E. coli* dry mass (BNID: 103904, Milo *et al.* (2010)), we estimate that $\approx 10^{10}$ carbon atoms must be brought into the cell in order to double all of the carbon-containing molecules (Figure 2(A, top)). Typical laboratory growth conditions, such as those explored in the aforementioned proteomic data sets, provide carbon as single class of sugar such as glucose, galactose, or xylose to name a few. *E. coli* has evolved myriad mechanisms by which these sugars can be transported across the cell membrane. One such mechanism of transport is via the PTS system which is a highly modular system capable of transporting a diverse range of sugars (Escalante *et al.*, 2012). The glucose-specific component of this system transports ≈ 200 glucose molecules per second per channel (BNID: 114686, Milo *et al.* (2010)). Making the assumption that this is a typical sugar transport rate, coupled with the need to transport 10^{10} carbon atoms, we arrive at the conclusion that on the order of 1000 transporters must be expressed in order to bring in enough carbon atoms to divide in 6000 s, diagrammed in the top panel of Figure 2(A). This estimate, along with the observed average number of carbohydrate transporters present in the proteomic data sets (Schmidt *et al.*, 2016; Peebo *et al.*, 2015; Valgepea *et al.*, 2013; Li *et al.*, 2014), is shown in Figure 2(A). While we estimate 1000 transporters are needed, the data reveals that at a division time of ≈ 6000 s there is nearly a ten-fold excess of transporters. Furthermore, the data illustrates that the average number of carbohydrate transporters present is largely-growth rate independent.

The estimate presented in Figure 2(A) neglects any specifics of the regulation of carbon transport system and presents a data-averaged view of how many carbohydrate transporters are present on average. Using the diverse array of growth conditions explored in the proteomic data sets, we can explore how individual carbon transport systems depend on the population growth rate. In Figure 2(B), we show the total number of carbohydrate transporters specific to different carbon sources. A striking observation, shown in the top-left plot of Figure 2(B), is the constancy in the expression of the glucose-specific transport systems (the PtsG enzyme of the PTS system and the glucose-transporting ManXYZ complex). Additionally, we note that the total number of glucose-specific transporters is tightly distributed $\approx 10^4$ per cell, an order of magnitude beyond the estimate shown in Figure 2(A). This illustrates that *E. coli* maintains a substantial number of complexes present for transporting glucose which is known to be the preferential carbon source (Monod, 1947; Liu *et al.*, 2005; Aidelberg *et al.*, 2014).

It is now understood that a large number of metabolic operons are regulated with dual-input logic gates that are only expressed when glucose concentrations are low (mediated by cyclic-AMP receptor protein CRP) and the concentration of other carbon sources are elevated (Gama-Castro *et al.*, 2016; Zhang *et al.*, 2014b). A famed example of such dual-input regulatory logic is in the regulation of the *lac* operon which is only natively activated in the absence of glucose and the presence of allolactose, an intermediate in lactose metabolism (Jacob and Monod, 1961), though we now know of many other such examples (Ireland *et al.*, 2020; Gama-Castro *et al.*, 2016; Belliveau *et al.*, 2018). This illustrates that once glucose is depleted from the environment, cells have a means to dramatically increase the abundance of the specific transporter needed to digest the next sugar

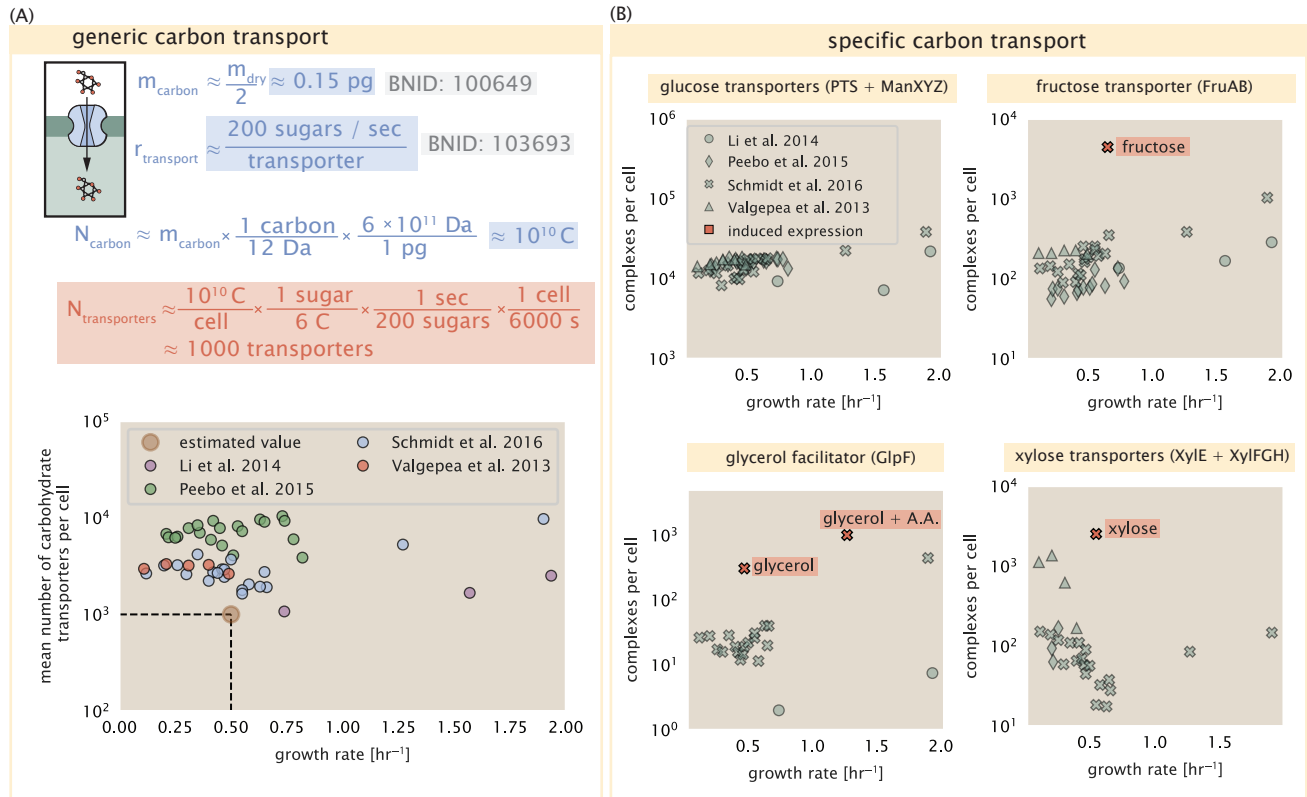


Figure 2. The abundance of carbon transport systems across growth rates. (A) A simple estimate for the minimum number of generic carbohydrate transport systems (top) assumes $\approx 10^{10}$ C are needed to complete division, each transported sugar contains ≈ 6 C, and each transporter conducts sugar molecules at a rate of ≈ 200 per second. Bottom plot shows the estimated number of transporters needed at a growth rate of ≈ 0.5 per hr (light-brown point and dashed lines). Colored points correspond to the mean number of carbohydrate transporters for different growth conditions across different published datasets. (B) The abundance of various specific carbon transport systems plotted as a function of the population growth rate. Red points and red-highlighted text indicate conditions in which the only source of carbon in the growth medium induces expression of the transport system.

that is present. Several examples of induced expression of a specific carbon-source transporters are shown in **Figure 2(B)**. Points colored in red (labeled by red text-boxes) correspond to growth conditions in which the specific carbon source (glycerol, xylose, or fructose) is present. These plots show that, in the absence of the particular carbon source, expression of the transporters is maintained on the order of $\sim 10^2$ per cell. However, when induced, the transporters become highly-expressed and are present on the order of $\sim 10^4$ per cell, which exceeds the generic estimate given in **Figure 2(A)**. Together, this generic estimation and the specific examples of induced expression suggest that transport of carbon across the cell membrane, while critical for growth, is not the rate-limiting step of cell division.

Phosphorus and Sulfur Transport

We now turn our attention towards other essential elements, namely phosphorus and sulfur. Phosphorus is critical to the cellular energy economy in the form of high-energy phosphodiester bonds making up DNA, RNA, and the XTP energy pool as well as playing a critical role in the post-translational modification of proteins and defining the polar-heads of lipids. In total, phosphorus makes up $\approx 3\%$ of the cellular dry mass which in typical experimental conditions is in the form of inorganic phosphate. The cell membrane has remarkably low permeability to this highly-charged and critical molecule, therefore requiring the expression of active transport systems. In *E. coli*, the proton electrochemical gradient across the inner membrane is leveraged to transport inorganic phosphate into the cell **Rosenberg et al. (1977)**. Proton-solute symporters are widespread in *E. coli* **Ramos and Kaback (1977)**; **Booth et al. (1979)** and can have rapid transport rates of 50 molecules per second for sugars and other solutes (BNID: 103159; 111777, **Milo et al. (2010)**). In *E. coli* the PitA phosphate transport system has been shown to very tightly coupled with the proton electrochemical gradient with a 1:1 proton:phosphate stoichiometric ratio (**Harris et al., 2001**; **Feist et al., 2007**). Illustrated in **Figure 3(A)**, we can estimate that ≈ 300 phosphate transporters are necessary to maintain an $\approx 3\%$ dry mass with a 6000 s division time. This estimate is again satisfied when we examine the observed copy numbers of PitA in proteomic data sets (plot in **Figure 3(A)**). While our estimate is very much in line with the observed numbers, we emphasize that this is likely a slight over estimate of the number of transporters needed as there are other phosphorous scavenging systems, such as the ATP-dependent phosphate transporter Pst system which we have neglected.

Satisfied that there are a sufficient number of phosphate transporters present in the cell, we now turn sulfur transport as another potentially rate limiting process. Similar to phosphate, sulfate is highly-charged not particularly membrane permeable, requiring active transport. While there exists a H⁺/sulfate symporter in *E. coli*, it is in relatively low abundance and is not well characterized (**Zhang et al., 2014a**). Sulfate is predominantly acquired via the ATP-dependent ABC transporter CysUWA system which also plays an important role in selenium transport (**Sekowska et al., 2000**; **Sirko et al., 1995**). While specific kinetic details of this transport system are not readily available, generic ATP transport systems in prokaryotes are on the order of 1 to 10 molecules per second (BNID: 109035, **Milo et al. (2010)**). Combining this generic transport rate, measurement of sulfur comprising 1% of dry mass, and a 6000 second division time yields an estimate of ≈ 1000 CysUWA complexes per cell (**Figure 3(B)**). Once again, this estimate is in notable agreement with proteomic data sets, suggesting that there are sufficient transporters present to acquire the necessary sulfur. In a similar spirit of our estimate of phosphorus transport, we emphasize that this is likely an over-estimate of the number of necessary transporters as we have neglected other sulfur scavenging systems that are in lower abundance.

Nitrogen Transport

Finally, we turn to nitrogen transport as the last remaining transport system highlighted in **Figure 1**. Unlike phosphate, sulfate, and various sugar molecules, nitrogen in the form of ammonia can readily diffuse across the cell membrane and has a permeability on par with water ($\approx 10^5$ nm/s, BNID:110824 **Milo et al. (2010)**). In particularly nitrogen-poor conditions, *E. coli* expresses a trans-

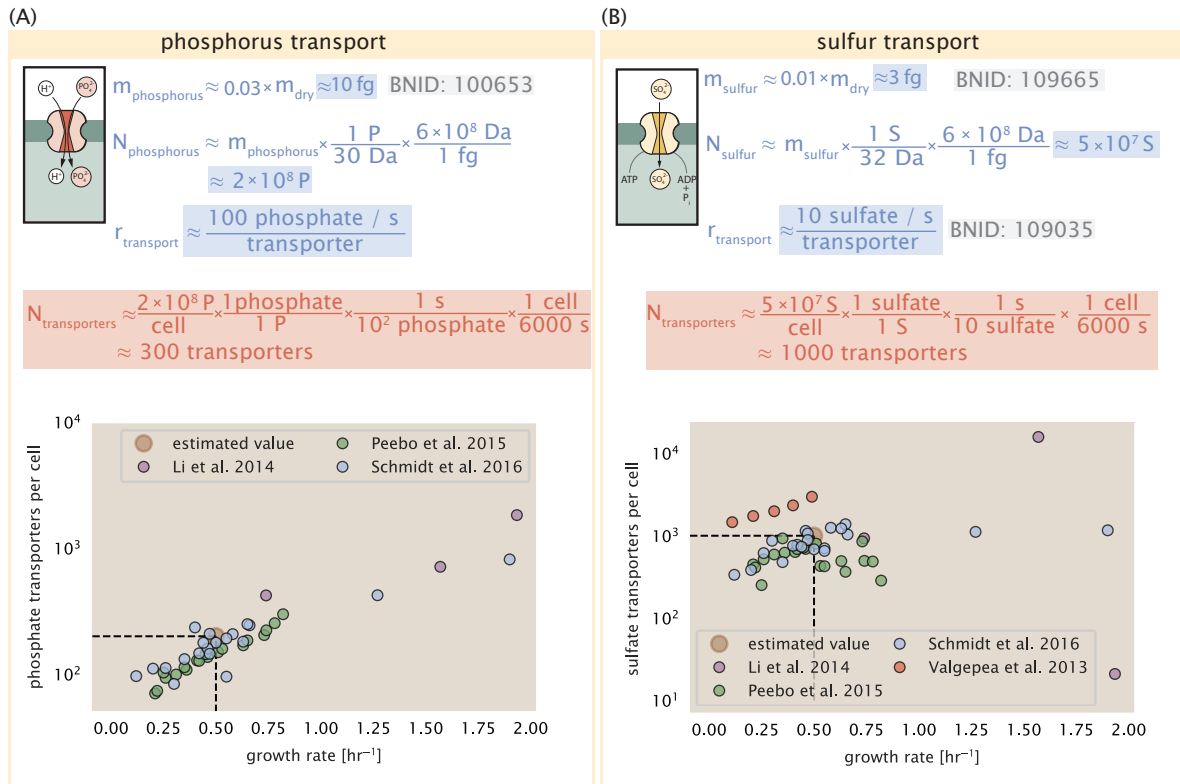


Figure 3. Estimates and measurements of phosphate and sulfate transport systems as a function of growth rate. (A) Estimate for the number of PitA phosphate transport systems needed to maintain a 3% phosphorus *E. coli* dry mass. Points in plot correspond to the the total number of PitA transporters per cell. (B) Estimate of the number of CysUWA complexes necessary to maintain a 1% sulfur *E. coli* dry mass. Points in plot correspond to average number of CysUWA transporter complexes that can be formed given the transporter stoichiometry $[\text{CysA}]_2[\text{CysU}][\text{CysW}][\text{Sbp/CysP}]$.

porter (AmtB) which appears to aid in nitrogen assimilation, though the mechanism and kinetic details of transport is still a matter of debate (*van Heeswijk et al., 2013; Khademi et al., 2004*). Beyond ammonia, another plentiful source of nitrogen come in the form of glutamate, which has its own complex metabolism and scavenging pathways. However, nitrogen is plentiful in the growth conditions examined in this work, permitting us to neglect nitrogen transport as a potential rate limiting process in cell division.

Energy Production

While the transport of nutrients is required to build new cell mass, the metabolic pathways involved in assimilation both consumes and generates energy in the form of NTPs. The high-energy phosphodiester bonds of (primarily) ATP power a variety of cellular processes that drive biological systems away from thermodynamic equilibrium. Our next class of estimates will consider the energy budget of a dividing cell in terms of the synthesis of ATP from ADP and inorganic phosphate as well as maintenance of the electrochemical proton gradient which powers it.

ATP Synthesis

Hydrolysis of the terminal phosphodiester bond of ATP forming ADP and an inorganic phosphate is kinetic driving force in a wide array of biochemical reactions. One such reaction is the formation of peptide bonds during translation which requires ≈ 2 ATPs for the charging of an amino acid to the tRNA and ≈ 2 ATP equivalents for the formation of the peptide bond between amino acids. Together, these energetic costs consume $\approx 80\%$ of the cells ATP budget (BNID: 107782; 106158; 101637; 111918, *Milo et al. (2010)*). The pool of ATP is produced by the F_1F_0 ATP synthase – a membrane-bound rotary motor which under ideal conditions can yield ≈ 300 ATP per second (BNID: 114701; *Milo et al. (2010); Weber and Senior (2003)*).

To estimate the total number of ATP equivalents consumed during a cell cycle, we will make the approximation that there are $\approx 3 \times 10^6$ proteins per cell with an average protein length of ≈ 300 peptide bonds (BNID: 115702; 108986; 104877, ?). Together, we arrive at the estimate that the typical *E. coli* cell consumes $\approx 5 \times 10^9$ ATP per cell cycle on protein synthesis alone and $\approx 6 \times 10^9$ ATP in total. Assuming that the ATP synthases are operating at their fastest possible rate, we arrive at an estimate that ≈ 3000 ATP synthases are needed to keep up with the energy demands of the cell. This estimate and a comparison with the data are shown in **Figure 4(A)**. Despite our assumption of maximal ATP production rate per synthase and approximation of all NTP consuming reactions being the same as ATP, we find that an estimate of a few thousand complete synthases per cell to agree well with the experimental data.

Generating the Proton Electrochemical Gradient

In order to produce ATP, the F_1F_0 ATP synthase itself must consume energy. Rather than burning through its own product, this intricate macromolecular machine has evolved to exploit the electrochemical potential established across the inner membrane through cellular respiration. This electrochemical gradient is manifest by the pumping of protons into the intermembrane space via the electron transport chains as they reduce NADH. In *E. coli*, this potential difference is ≈ -200 mV (BNID: 102120, *Milo et al. (2010)*). As estimated in the supporting information, this potential difference is generated by maintaining $\approx 2 \times 10^4$ protons in the intermembrane space.

However, the constant rotation of the ATP synthases would rapidly abolish this potential difference if it were not being actively maintained. To undergo a complete rotation (and produce a single ATP), the F_1F_0 ATP synthase must shuttle ≈ 4 protons across the membrane into the cytosol (BNID: 103390, *Milo et al. (2010)*). With ≈ 3000 ATP synthases each generating 300 ATP per second, the 2×10^4 protons establishing the 200 mV potential would consumed in only a few milliseconds! This brings us to our next estimate: how many electron transport complexes are needed to support the consumption rate of the ATP synthases?

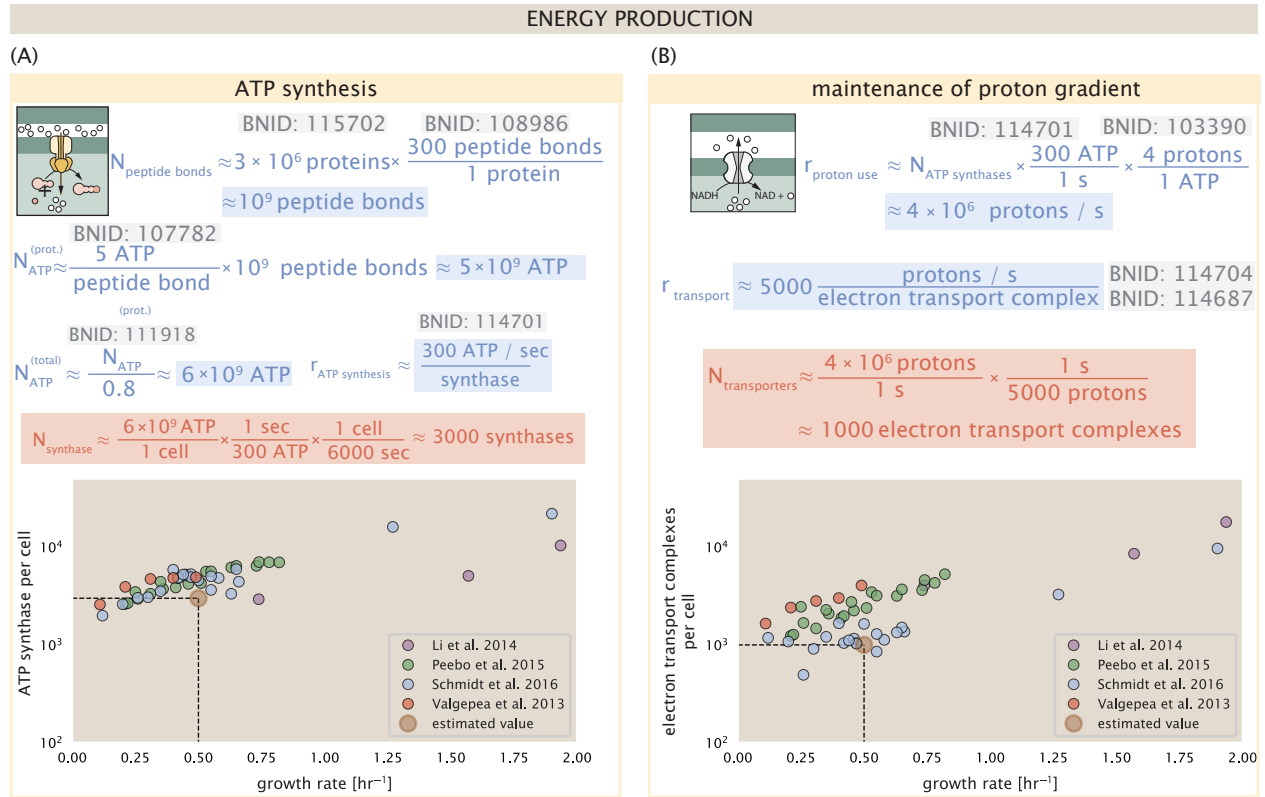


Figure 4. The abundance of F_1 - F_0 ATP synthases and electron transport chain complexes as a function of growth rate. (A) Estimate of the number of F_1 - F_0 ATP synthase complexes needed to accommodate peptide bond formation and other NTP dependent processes. Points in plot at bottom correspond to the mean number of complete F_1 - F_0 ATP synthase complexes that can be formed given proteomic measurements and the subunit stoichiometry [AtpE]₁₀[AtpF]₂[AtpB]₃[AtpC]₃[AtpH]₃[AtpA]₃[AtpG]₃[AtpD]₃. (B) Estimate of the number of electron transport chain complexes needed to maintain a membrane potential of -200 mV given estimate of number of F_1 - F_0 ATP synthases from (A). Points in plot correspond to the average number of complexes identified as being involved in aerobic respiration by the Gene Ontology identifier GO:0019646 that could be formed given proteomic observations. These complexes include cytochromes *bd1* ([CydA][CydB][CydX][CydH]), *bdII* ([AppC][AppB]), *bo3*, ([CyoD][CyoA][CyoB][CyoC]) and NADH:quinone oxidoreductase I ([NuoA][NuoH][NuoJ][NuoK][NuoL][NuoM][NuoN][NuoB][NuoC][NuoE][NuoF][NuoG][NuoI]) and II ([Ndh]).

The electrochemistry of the electron transport complexes of *E. coli* have been the subject of intense biochemical and biophysical study over the past half century (Ingledew and Poole, 1984; Khademian and Imlay, 2017; Cox et al., 1970; Henkel et al., 2014). A recent work (Szenk et al., 2017) examined the respiratory capacity of the *E. coli* electron transport complexes using structural and biochemical data revealing that each electron transport chain rapidly pumps protons into the intermembrane space at a clip of ≈ 5000 protons per second (BNID: 114704; 114687, Milo et al. (2010)). Using our estimate of the number of ATP synthases required per cell (Figure 4(A)), coupled with these recent measurements, we estimate that ≈ 1000 electron transport complexes would be necessary to facilitate the $\approx 4 \times 10^6$ protons per second diet of the cellular ATP synthases. This estimate is in agreement with the number of complexes identified in the proteomic datasets (plot in Figure 4(B)).

[GC: I think we really need to comment on the growth rate dependence here and see if we can make any sense of it with increasing surface area.]

References

- Aidelberg, G., Towbin, B. D., Rothschild, D., Dekel, E., Bren, A., and Alon, U. (2014). Hierarchy of non-glucose sugars in *Escherichia coli*. *BMC Systems Biology*, 8(1):133.
- Antonenko, Y. N., Pohl, P., and Denisov, G. A. (1997). Permeation of ammonia across bilayer lipid membranes studied by ammonium ion selective microelectrodes. *Biophysical Journal*, 72(5):2187–2195.
- Assentoft, M., Kaptan, S., Schneider, H.-P., Deitmer, J. W., de Groot, B. L., and MacAulay, N. (2016). Aquaporin 4 as a NH₃ Channel. *Journal of Biological Chemistry*, 291(36):19184–19195.
- Bauer, S. and Ziv, E. (1976). Dense growth of aerobic bacteria in a bench-scale fermentor. *Biotechnology and Bioengineering*, 18(1):81–94. [_eprint: https://onlinelibrary.wiley.com/doi/pdf/10.1002/bit.260180107](https://onlinelibrary.wiley.com/doi/pdf/10.1002/bit.260180107).
- Belliveau, N. M., Barnes, S. L., Ireland, W. T., Jones, D. L., Sweredoski, M. J., Moradian, A., Hess, S., Kinney, J. B., and Phillips, R. (2018). Systematic approach for dissecting the molecular mechanisms of transcriptional regulation in bacteria. *Proceedings of the National Academy of Sciences*, 115(21):E4796–E4805.
- Booth, I. R., Mitchell, W. J., and Hamilton, W. A. (1979). Quantitative analysis of proton-linked transport systems. The lactose permease of *Escherichia coli*. *Biochemical Journal*, 182(3):687–696.
- Cox, G. B., Newton, N. A., Gibson, F., Snoswell, A. M., and Hamilton, J. A. (1970). The function of ubiquinone in *Escherichia coli*. *Biochemical Journal*, 117(3):551–562.
- Escalante, A., Salinas Cervantes, A., Gosset, G., and Bolívar, F. (2012). Current knowledge of the *Escherichia coli* phosphoenolpyruvate–carbohydrate phosphotransferase system: Peculiarities of regulation and impact on growth and product formation. *Applied Microbiology and Biotechnology*, 94(6):1483–1494.
- Feist, A. M., Henry, C. S., Reed, J. L., Krummenacker, M., Joyce, A. R., Karp, P. D., Broadbelt, L. J., Hatzimanikatis, V., and Palsson, B. Ø. (2007). A genome-scale metabolic reconstruction for *Escherichia coli* K-12 MG1655 that accounts for 1260 ORFs and thermodynamic information. *Molecular Systems Biology*, 3(1):121.
- Gama-Castro, S., Salgado, H., Santos-Zavaleta, A., Ledezma-Tejeda, D., Muñoz-Rascado, L., García-Sotelo, J. S., Alquicira-Hernández, K., Martínez-Flores, I., Pannier, L., Castro-Mondragón, J. A., Medina-Rivera, A., Solano-Lira, H., Bonavides-Martínez, C., Pérez-Rueda, E., Alquicira-Hernández, S., Porrón-Sotelo, L., López-Fuentes, A., Hernández-Koutoucheva, A., Moral-Chávez, V. D., Rinaldi, F., and Collado-Vides, J. (2016). RegulonDB version 9.0: High-level integration of gene regulation, coexpression, motif clustering and beyond. *Nucleic Acids Research*, 44(D1):D133–D143.
- Harris, R. M., Webb, D. C., Howitt, S. M., and Cox, G. B. (2001). Characterization of PitA and PitB from *Escherichia coli*. *Journal of Bacteriology*, 183(17):5008–5014.
- Heldal, M., Norland, S., and Tumyr, O. (1985). X-ray microanalytic method for measurement of dry matter and elemental content of individual bacteria. *Applied and Environmental Microbiology*, 50(5):1251–1257.
- Henkel, S. G., Beek, A. T., Steinsiek, S., Stagge, S., Bettenbrock, K., de Mattos, M. J. T., Sauter, T., Sawodny, O., and Ederer, M. (2014). Basic Regulatory Principles of *Escherichia coli*'s Electron Transport Chain for Varying Oxygen Conditions. *PLoS ONE*, 9(9):e107640.
- Ingledeu, W. J. and Poole, R. K. (1984). The respiratory chains of *Escherichia coli*. *Microbiological Reviews*, 48(3):222–271.
- Ireland, W. T., Beeler, S. M., Flores-Bautista, E., Belliveau, N. M., Sweredoski, M. J., Moradian, A., Kinney, J. B., and Phillips, R. (2020). Deciphering the regulatory genome of *Escherichia coli*, one hundred promoters at a time. *bioRxiv*.
- Jacob, F. and Monod, J. (1961). Genetic regulatory mechanisms in the synthesis of proteins. *Journal of Molecular Biology*, 3(3):318–356.
- Jun, S., Si, F., Pugatch, R., and Scott, M. (2018). Fundamental principles in bacterial physiology - history, recent progress, and the future with focus on cell size control: A review. *Reports on Progress in Physics*, 81(5):056601.
- Khademi, S., O'Connell, J., Remis, J., Robles-Colmenares, Y., Miercke, L. J. W., and Stroud, R. M. (2004). Mechanism of Ammonia Transport by Amt/MEP/Rh: Structure of AmtB at 1.35 Å. *Science*, 305(5690):1587–1594.
- Khademian, M. and Imlay, J. A. (2017). *Escherichia Coli* cytochrome c peroxidase is a respiratory oxidase that enables the use of hydrogen peroxide as a terminal electron acceptor. *Proceedings of the National Academy of Sciences*, 114(33):E6922–E6931.

- Li, G.-W., Burkhardt, D., Gross, C., and Weissman, J. S. (2014). Quantifying absolute protein synthesis rates reveals principles underlying allocation of cellular resources. *Cell*, 157(3):624–635.
- Liu, M., Durfee, T., Cabrera, J. E., Zhao, K., Jin, D. J., and Blattner, F. R. (2005). Global Transcriptional Programs Reveal a Carbon Source Foraging Strategy by *Escherichia coli*. *Journal of Biological Chemistry*, 280(16):15921–15927.
- Milo, R., Jorgensen, P., Moran, U., Weber, G., and Springer, M. (2010). BioNumbers—the database of key numbers in molecular and cell biology. *Nucleic Acids Research*, 38(suppl_1):D750–D753.
- Monod, J. (1947). The phenomenon of enzymatic adaptation and its bearings on problems of genetics and cellular differentiation. *Growth Symposium*, 9:223–289.
- Neidhardt, F. C., Ingraham, J., and Schaechter, M. (1991). *Physiology of the Bacterial Cell - A Molecular Approach*, volume 1. Elsevier.
- Peebo, K., Valgepea, K., Maser, A., Nahku, R., Adamberg, K., and Vilu, R. (2015). Proteome reallocation in *Escherichia coli* with increasing specific growth rate. *Molecular BioSystems*, 11(4):1184–1193.
- Ramos, S. and Kaback, H. R. (1977). The relation between the electrochemical proton gradient and active transport in *Escherichia coli* membrane vesicles. *Biochemistry*, 16(5):854–859.
- Rosenberg, H., Gerdes, R. G., and Chegwidden, K. (1977). Two systems for the uptake of phosphate in *Escherichia coli*. *Journal of Bacteriology*, 131(2):505–511.
- Schaechter, M., Maaløe, O., and Kjeldgaard, N. O. (1958). Dependency on medium and temperature of cell size and chemical composition during balanced growth of *Salmonella typhimurium*. *Microbiology*, 19(3):592–606.
- Schmidt, A., Kochanowski, K., Vedelaar, S., Ahrné, E., Volkmer, B., Callipo, L., Knoop, K., Bauer, M., Aebersold, R., and Heinemann, M. (2016). The quantitative and condition-dependent *Escherichia coli* proteome. *Nature Biotechnology*, 34(1):104–110.
- Sekowska, A., Kung, H.-F., and Danchin, A. (2000). Sulfur Metabolism in *Escherichia coli* and Related Bacteria: Facts and Fiction. *Journal of Molecular Microbiology and Biotechnology*, 2(2):34.
- Sirko, A., Zatyka, M., Sadowy, E., and Hulanicka, D. (1995). Sulfate and thiosulfate transport in *Escherichia coli* K-12: Evidence for a functional overlapping of sulfate- and thiosulfate-binding proteins. *Journal of Bacteriology*, 177(14):4134–4136.
- Stasi, R., Neves, H. I., and Spira, B. (2019). Phosphate uptake by the phosphonate transport system PhnCDE. *BMC Microbiology*, 19.
- Szenk, M., Dill, K. A., and de Graff, A. M. R. (2017). Why Do Fast-Growing Bacteria Enter Overflow Metabolism? Testing the Membrane Real Estate Hypothesis. *Cell Systems*, 5(2):95–104.
- Taymaz-Nikerel, H., Borujeni, A. E., Verheijen, P. J. T., Heijnen, J. J., and van Gulik, W. M. (2010). Genome-derived minimal metabolic models for *Escherichia coli* MG1655 with estimated in vivo respiratory ATP stoichiometry. *Biotechnology and Bioengineering*, 107(2):369–381. [_eprint: https://onlinelibrary.wiley.com/doi/pdf/10.1002/bit.22802](https://onlinelibrary.wiley.com/doi/pdf/10.1002/bit.22802).
- Valgepea, K., Adamberg, K., Seiman, A., and Vilu, R. (2013). *Escherichia coli* achieves faster growth by increasing catalytic and translation rates of proteins. *Molecular BioSystems*, 9(9):2344.
- van Heeswijk, W. C., Westerhoff, H. V., and Boogerd, F. C. (2013). Nitrogen Assimilation in *Escherichia coli*: Putting Molecular Data into a Systems Perspective. *Microbiology and Molecular Biology Reviews*, 77(4):628–695.
- Weber, J. and Senior, A. E. (2003). ATP synthesis driven by proton transport in F1F0-ATP synthase. *FEBS Letters*, 545(1):61–70.
- Willisky, G. R., Bennett, R. L., and Malamy, M. H. (1973). Inorganic Phosphate Transport in *Escherichia coli*: Involvement of Two Genes Which Play a Role in Alkaline Phosphatase Regulation. *Journal of Bacteriology*, 113(2):529–539.
- Zhang, L., Jiang, W., Nan, J., Almqvist, J., and Huang, Y. (2014a). The *Escherichia coli* CysZ is a pH dependent sulfate transporter that can be inhibited by sulfite. *Biochimica et Biophysica Acta (BBA) - Biomembranes*, 1838(7):1809–1816.
- Zhang, Z., Aboulwafa, M., and Saier, M. H. (2014b). Regulation of *crp* Gene Expression by the Catabolite Repressor/Activator, Cra, in *Escherichia coli*. *Journal of Molecular Microbiology and Biotechnology*, 24(3):135–141.